

**MSEC2012-7291**

## **DEVELOPMENT OF A FIBER ORIENTATION MEASUREMENT METHODOLOGY FOR INJECTION MOLDED THERMALLY-ENHANCED POLYMERS**

**Timothy Hall**

Department of Mechanical Engineering  
University of Maryland  
College Park, MD 20742, USA  
Email: timrhall@umd.edu

**Hugh A. Bruck**

Department of Mechanical Engineering  
& Multiscale Measurements Laboratory  
University of Maryland  
College Park, MD 20742, USA  
Email: bruck@umd.edu

**Arumugham Vaishnavi Subramoniam**

Department of Mechanical Engineering  
University of Maryland  
College Park, MD 20742, USA  
Email: avsubram@gmail.com

**Satyandra K. Gupta**

Department of Mechanical Engineering  
& Institute for Systems Research  
University of Maryland  
College Park, MD 20742, USA  
Email: skgupta@umd.edu

### **ABSTRACT**

*Thermally-enhanced polymer composites are a promising alternative to exotic metals in seawater heat exchanger applications due to the low cost and corrosion resistance of base polymers and heat transfer rates competitive with corrosion-resistant metals such as titanium or stainless steel. While the properties of thermally-enhanced polymer composites are well-suited for heat exchanger applications, fiber orientation has a strong influence on the structural and thermal performance of the manufactured components. In this study, a method of creating samples, sectioning and polishing them for imaging, microscope sampling for the identification of fibers, image processing to characterize fiber orientation, and finally comparison to predictions from computer-aided engineering (CAE) software is demonstrated for collecting experimental information on fiber orientation of molded parts. Understanding fiber orientation in injection-molded polymer heat exchangers is important for ensuring ideal heat transfer and structural performance and this study presents an experimental methodology for determining the influence of injection molding process parameters on fiber orientation in thermally-enhanced polymer composite geometries.*

### **1 INTRODUCTION**

The utilization of polymers in heat exchangers is attractive due to their relatively low cost and weight, lower fabrication energy and lifecycle energy use than equivalent metal heat exchangers [1], and corrosion and fouling resistance [2]. The introduction of new thermally-enhanced polymer composites and manufacturing processes has led to renewed interest in polymer heat exchangers and emerging applications previously supported only by heat exchangers made of exotic metallic alloys. Industrial applications which utilize seawater as a cooling medium for heat exchangers traditionally require exotic alloys to survive the corrosive environment, leading to dramatically increased costs and processing requirements. Polymer composites utilizing thermally-enhanced fillers, such as pitch-based carbon fiber, have led to orders of magnitude improvement in overall thermal conductivity, making them competitive with corrosion-resistant metals such as titanium and copper-nickel alloys. [3]

In thermally-enhanced and other fiber-filled composites, fiber orientation can play an important role in determining the material properties of created parts. Thermally-enhanced fibers exhibit thermal and structural properties that are order of magnitudes higher along the length of the fiber compared to transverse to the length of the fiber. Therefore fiber alignment can lead

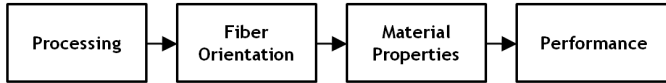


**FIGURE 1:** The effect of processing parameters on part performance due to fiber orientation.

to anisotropic material properties that must be accounted for in the design stage. In injection molded parts, many factors affect fiber alignment, including the geometry of the part and injection molding processing parameters, such as melt flow rate. Figure 1 below demonstrates the fiber orientation process that must be understood in order to properly design for fiber orientation in injection molded parts in order to reach desired performance goals.

Using finite element analysis to estimate fiber orientation has been well developed for traditional polymer composites and is integrated with the industry-leading injection molding simulation environment Moldflow®. The basis for this analysis is primarily the Folgar-Tucker model, developed as a process of modeling fiber orientation and how competing phenomena in injection molding affect it. This model has been rigorously tested and reinforced with experimental findings for traditional polymer composites but it is useful to study the utility of this model in new thermally-enhanced composites.

This paper presents a methodology for collecting and analyzing samples to determine fiber orientation in relatively large sections and develop both a qualitative and quantitative comparison to Moldflow® predictions. While this approach is not necessarily new, the goal of developing a more global understanding of fiber orientation in sample parts is generally counter to the recent progression of more precise and intricate measurement of fiber orientation that is not suitable for rapid testing and large test regions.

## 2 RELATED WORK

### 2.1 Fiber Orientation

The Folgar-Tucker model for fiber orientation in concentrated suspensions, [4], provides the foundation for predicting fiber orientation in injection molding. This model uses parameters such as shear stress, viscosity, and velocity flow field to determine how fiber align as the injection molding process progresses. This model has been rigorously studied and is the accepted prediction method in industry-standard injection molding simulation tools such as Moldflow®.

This model, in its most frequently used form, utilizes tensors to provide a compact representation of fiber orientation [5]. Fundamentally, each fiber is represented as a vector,  $\mathbf{p}$ , with two angles,  $\theta$  and  $\phi$ , as shown in Figure 2. The vector components can be found using this representation with Equation 1, shown below.

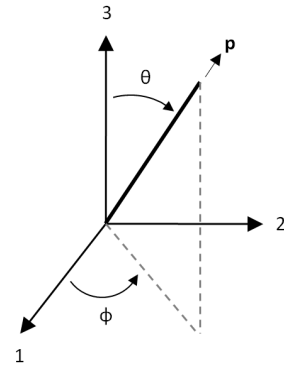


**FIGURE 2:** Vector representing fiber orientation.

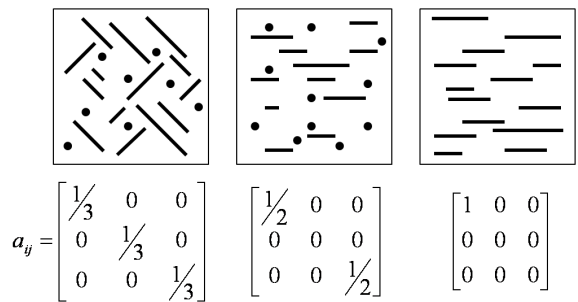


**FIGURE 3:** Example tensor values.

$$\begin{aligned} p_1 &= \sin \theta \cos \phi \\ p_2 &= \sin \theta \sin \phi \\ p_3 &= \cos \theta \end{aligned} \quad (1)$$

With each fiber defined as a vector, the most common representation of fiber orientation is the probability distribution function for orientation,  $\psi$ . This distribution is then presented concisely as a second-order tensor using Equation 2 over all directions. The tensor value represents the overall orientation distribution of a sample region and Figure 3 demonstrates some example tensor values.

$$a_{ij} = \oint p_i p_j \psi(\mathbf{p}) d\mathbf{p} \quad (2)$$

While some fiber measurement schemes use three-dimensional information to determine fiber orientation [6, 7], the majority of methods utilize imaging two-dimensional cross-sections and determining fiber orientation from these sections.

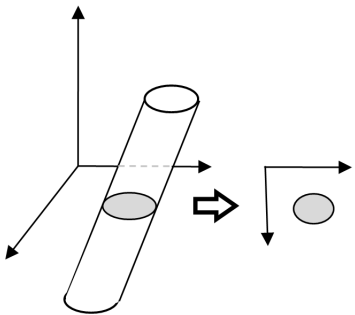


**FIGURE 4:** Fiber cross-section for determining orientation.

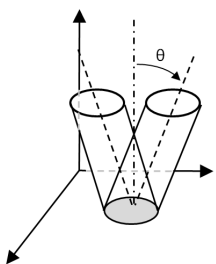


**FIGURE 5:** Issue resolving sign of out-of-plane angle using simple cross-section.

Using the fundamental geometry of fibers and the vector representation described previously, the fiber orientation of a given fiber can be determined based on the dimensions of the elliptical cross-section, shown in Figure 4, and is detailed in Section 4.4. While this method is very useful for determining fiber orientation from simple cross-sections, there exists ambiguity in determining the out-of-plane angle for a given cross-section, as shown in Figure 5. This affects values for two of the six tensor components,  $a_{13}$  and  $a_{23}$ , and should be taken into consideration when evaluating fiber orientation measurements.

## 2.2 Experimental Methodologies

Much work has been done on developing methodologies for increasingly more accurate measurement of fiber orientation in test samples. There are three primary components of experimental measurement that have received significant attention: sectioning techniques, imaging methods, and image processing algorithms.

**Sectioning Techniques.** The development of sectioning techniques has progressed primarily with the goal of providing the most useful information for image processing. Initial methods used sectioning and polishing technologies from traditional experimental applications and used single sections of a region of interest to develop an understanding of the accuracy of fiber orientation predictions for the sample [8, 9].

The progression from this simple sectioning technique has generally been used to develop a more accurate three-dimensional representation of fiber orientation by using methods such as multiple slice sections or sections at multiple angles. Using multiple slices that are minimal thickness apart allows the direction of fibers to be tracked and used to accurately determine the out-of-plane orientation components [10–12]. While this method offers more precision with a fully-resolved 3D orientation, it is a more intensive process due to its requirements for aligning the results from the multiple sections through the use of complex registration schemes or other alignment methods. Using sections at multiple angles can provide significant information for determining fiber orientation and allows a much better understanding of how fiber orientation changes throughout the sample [13]. While this is valuable, preparing multiple sections introduces significant complexity and labor into the experimental process and may limit the size of sections and therefore the useful area that can be studied.

**Imaging Methods.** With the sample geometry sectioned and polished for imaging, there are many options that have been explored for measuring fibers in a test section. The original and most common method is optical microscopy [10, 12, 13]. This method is attractive due to its high availability and lack of complexity for quickly implementing sampling methodologies but its primary drawback is that it is difficult to measure out-of-plane orientation components due to the strictly two-dimensional imaging behavior, although this has been resolved through the use of advanced sectioning methods.

Other imaging methods that have been investigated include X-rays [14], Scanning electron microscopy [15, 16], and confocal microscopy [17]. X-ray imaging is potentially useful for nondestructive testing but often requires complex sectioning for useful results and may require substitution of materials that are readily X-ray compatible. Scanning electron microscopy provides a remarkably detailed image of fiber orientation and through advanced methods, such as Shadow SEM Analysis [16], out-of-plane orientation can be determined using a single section. Unfortunately the high magnification utilized in SEM analysis is not suitable for measuring fiber orientation over large sample sections. Confocal microscopy uses clever imaging techniques to extract three-dimensional orientation information from two-dimension images and is therefore useful for single sectioning methods but it lacks availability and may be too complex for general experimental usage.

**Image Processing Algorithms.** Initial image processing techniques often used manual fiber identification [13] for processing but more powerful computing platforms and image processing techniques have dramatically advanced the process and led to significant automation. The ability to sample large areas was improved with the use of image analysis tools to align and order sequentially collected images and the ability to analyze fiber orientation in real time [10]. Recent work has led to in-

tricate identification and visualization of the three-dimensional fiber orientation of test samples [6] and represents the advancing accuracy of fiber orientation measurement.

### 3 PROBLEM DEFINITION

Based on the progress that has occurred in developing experimental methods for measuring fiber orientation, and the various advantages and limitations that are associated with them, along with the specific motivation for this project, the following goals were identified for developing the experimental methodology for this study:

1. **Low Magnification:** Use standard, relatively low-magnification, light microscopy to collect image samples due to its high availability and ability to sample large test sections.
2. **Single Sample Section:** Use a single section and standard polishing technique to prepare samples for imaging to ensure that the process can be applied to a large variety of materials and reduce the complexity of preparing samples.
3. **Use Goal Material:** Use the target material for the sample geometry in its applied form rather than specially-designed materials with tracers or other unique fillers so that results represent the behavior of the final product.
4. **Control Tensor Region:** Provide granular control of the tensor calculation region size in order to provide both global and local representation of the fiber orientation across the sample geometry.
5. **Standardized Tools:** Use standardized image processing and tensor calculation techniques to take advantage of common understanding and build upon established methods.

### 4 APPROACH

The approach developed for this project is divided into two primary sections: the experimental setup for collecting fiber orientation information and the image processing framework for interpreting the found fiber orientation information. The presented approach presents the experimental procedure required to compare the fiber orientation information for a sample geometry to simulation predictions using both qualitative and quantitative methods.

#### 4.1 Experimental Setup

**Sectioning and Polishing.** Due to the destructive nature and labor intensity of sectioning samples, a single sample section methodology was chosen for this study. Therefore, careful consideration must be given to selecting a sample section that will provide the most useful information about the fiber orientation behavior in a sample geometry. For methods where large areas can be sampled, the section that gives that largest sample

region may be the best choice although any particular regions of interest should be accounted for. Traditionally, small test regions are selected to measure the fiber orientation in a particular location while large test regions can be used to analyze more complex behavior, such as how far from the injection location that fibers reach a certain level of alignment, and other properties that contribute to a more global understanding of the fiber orientation in a test part. After selecting a suitable test section, a grinding and polishing procedure is used to prepare the test sample. This procedure was developed following traditional best practices, designed to use standard polishing equipment, and was formulated based on the work of [18] and [19] to ensure a uniform, highly polished section for microscope imaging.

**Microscope Imaging.** The microscope chosen for this approach was a traditional light microscope with polarizing filter technology. Reflected light was chosen to alleviate the need for thin slices that are required for transmitted light. The polarizing filters were used to take advantage of the differing characteristics of the fibers and the surrounding matrix material, and were adjusted to reinforce the reflected light from the fibers and light absorbed in the polymer matrix. This method was shown to produce high contrast for carbon fiber filled polymer composites and should be useful for most fiber-filled polymers with significant differences between the fiber and matrix materials. A relatively low magnification of 5x was chosen to provide a clear picture of the fibers in the matrix while providing a wide enough view in order to sample large sections.

#### 4.2 Fiber Orientation Comparison Framework

A fiber orientation comparison framework was developed to take large sample sections consisting of many microscope images, analyze and determine fiber orientation for the entire sample, and then compare these results with simulation predictions. Details of this process include the goal of controlling the examined size for making fiber orientation measurements and developing both a local and global understanding of fiber orientation for comparison to predicted values. This framework progresses as a six-step process and is presented below.

**Step 1. Initialization.** The initialization stage is primarily used to define the connection to microscope images and customize image processing settings for the particular application. It is also used to define the relationships between the microscope images and how they correspond to the overall test section to ensure the individual results properly correlate to the overall behavior.

**Step 2. Perform Image Processing on Original Images.** Image processing, detailed in Section 4.3, is applied to all of the original microscope images to extract raw orientation information for all of the fibers found in each image.

**Step 3. Combine Image Results and Subdivide into Tensor Regions.** With the raw fiber orientation information found

for each image, the results are combined to form the overall sample section. This includes cropping original images to remove any overlap or other requirements for resizing and arranging results information to properly correspond with positioning in the test section.

With the sample section reconstructed from its component images, it is then subdivided into regions for tensor analysis. This method was chosen instead of using the original image regions to calculate tensor values in order to provide more control of the tensor region size. This control over the resolution of measured tensor values allows better comparison to predicted values due to the ability to find both local and global information using high-resolution and low-resolution tensor regions, respectively. It can also be used for measurement quality control such as ensuring there is sufficient fiber information in a selected tensor region for accurately determining tensor values.

**Step 4. Calculate Tensor Values.** Using the defined tensor regions, tensor values are calculated to represent fiber orientation, described in Section 4.4.

**Step 5. Subdivide Simulation Results and Sample Tensor Values.** Using the same defined tensor regions as the experimental results, subdivide the simulation results. The tensor values are then sampled in these tensor regions to determine the tensor values corresponding to the found experimental values. The simulation results present the tensor components as a continuous value across the tensor region so a representative tensor value is found by sampling multiple points within the tensor region and determining the average tensor value for each region to compare with the measured experimental values.

**Step 6. Compare Experimental and Simulation Tensor Values.** With both measured experimental tensor values and predicted tensor values, the fiber orientation information is compared across the sample section, shown in Section 4.5.

### 4.3 Image Processing Algorithm

The image processing algorithm was developed using open-source tools (OpenCV) and standard techniques to build upon a common and well-developed foundation for the image processing framework and allow wide availability for potential applications. Additionally, the algorithm was designed to be flexible to changing sample materials that can lead to varying contrast between fiber and matrix materials, fiber size, and other properties to ensure that the goal materials for varying applications can be used. The steps below outline the major stages of the developed image processing algorithm.

**Step 1. Resizing, Down Sampling, and Smoothing.** This step is used to define a common set of input image parameters and prepare the raw microscope image for processing. The image resizing and down sampling (performed via Gaussian Pyramidal decomposition) are used to ensure that the measured fibers are within a defined general size for consistent processing in sub-

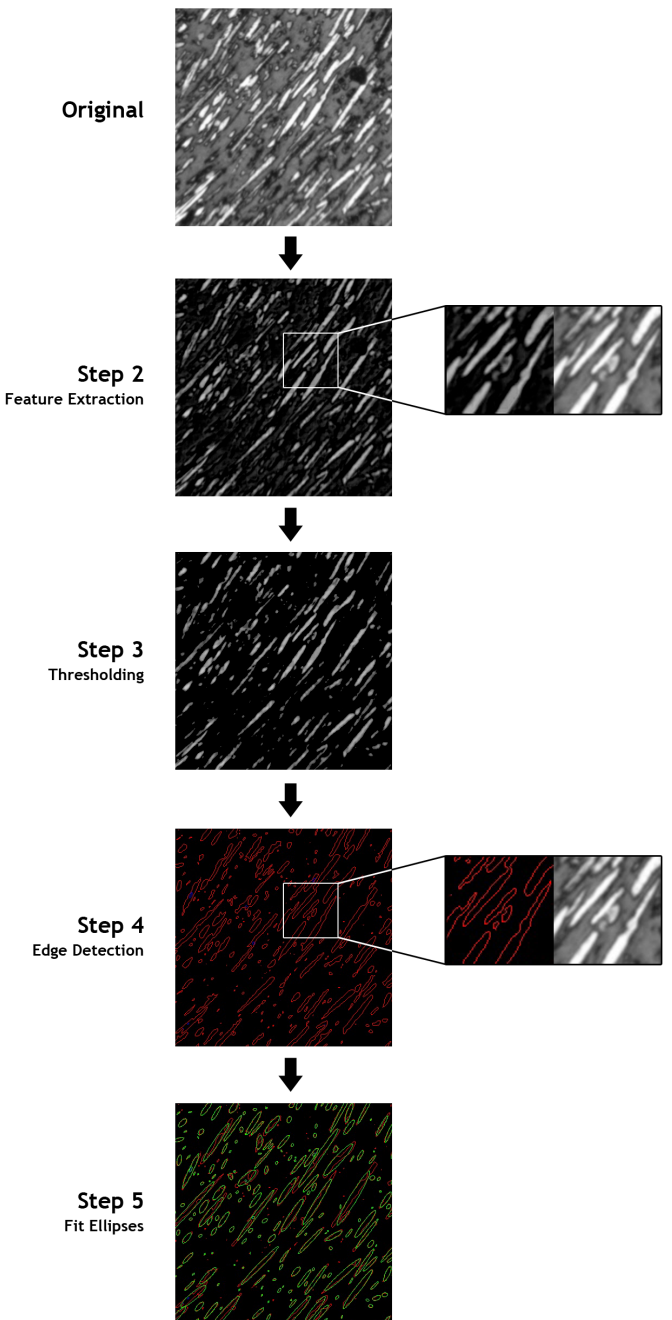


**FIGURE 6:** Progression of image processing algorithm for identifying fibers, described in Section 4.3.

sequent steps. The smoothing is performed to remove noise that can be introduced from the microscope and camera system.

**Step 2. Feature Extraction.** To better differentiate between fibers and the surrounding matrix material, feature extraction is performed on the prepared microscope image. This process, de-

veloped in the field of mathematical morphology and known as a top-hat transformation, uses a defined structuring element to explore the image to find areas that the structuring element fits into that are brighter than their surroundings. The structuring element is sized so that it is smaller than the general fiber size and isolates the fibers from the dark matrix background.

**Step 3. Thresholding.** With the fibers well defined from the background material, a thresholding operation is applied to separate the image into light areas representing fibers and dark areas representing the matrix material. After the thresholding application is complete, the areas of the image that contains fibers have a value of 1 and all other areas are 0, allowing for more precise application of image processing techniques in the following steps.

**Step 4. Edge and Shape Detection.** Edge detection is then applied to identify all of the transition regions between fiber and matrix values. Shape detection is then used to locate continuous edges, saving each contour as a sequence of points.

**Step 5. Fit Ellipses to Detected Shapes.** Finally, each contour is processed and if it has greater than six points a two-dimensional box is fit such that it is the minimal size containing the contour and is represented by an ellipse for the processed image. Each ellipse denotes a fiber found in the processed image and its geometrical properties are saved for use in calculating the fiber orientation information for the sample.

Using the developed image processing algorithm, the supplied microscope image is analyzed and each fiber is isolated and marked with an ellipse. This set of ellipses representing the found fibers is the output of the algorithm and contains the geometric information necessary for calculating fiber orientation tensor values for the measured area.

#### 4.4 Tensor Calculation

With the set of ellipses representing the found fibers from the image processing analysis, the fiber orientation tensors for a defined region can be calculated. Using the ellipse formulation shown in Figure 7, the required ellipse properties, such as minor and major axis length ( $m$  and  $M$ , respectively), can be calculated using Equations 3-5.

$$m = \sqrt{(x_3 - x_4)^2 + (y_3 - y_4)^2} \quad (3)$$

$$X = x_2 - x_1, Y = y_2 - y_1 \quad (4)$$

$$M = \sqrt{X^2 + Y^2} \quad (5)$$

With each fiber fully defined as an ellipse, the tensor values can be calculated for the fibers contained within a specified region using Equations 6 and 7 and Table 1. In Equation 6,  $a_{ij}$  represents the overall tensor component for the region, and  $(a_{ij})_n$  represents the tensor component for the  $n$ th fiber (shown in Table 1).  $F_n$  is a weighting function used to cope with the biasing

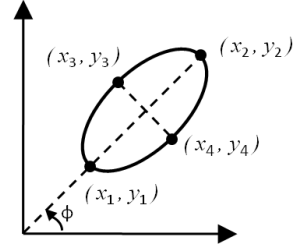


**FIGURE 7:** Elliptical fiber cross-section for determining orientation.

that can occur due to fibers lying predominantly perpendicular to the sample section being more likely to appear in the specified region.

$$a_{ij} = \frac{\sum (a_{ij})_n F_n}{\sum F_n} \quad (6)$$

$$F_n = \frac{M_n}{m_n} \quad (7)$$

**TABLE 1:** Tensor components for a single fiber.

Tensor component for $n$ th fiber	Representation with measured geometrical parameters
$(a_{11})_n$	$X^2 \left( \frac{1}{M^2} - \frac{m^2}{M^4} \right)$
$(a_{12})_n = (a_{21})_n$	$XY \left( \frac{1}{M^2} - \frac{m^2}{M^4} \right)$
$(a_{13})_n = (a_{31})_n$	$X \sqrt{\frac{m^2}{M^4} - \frac{m^4}{M^6}}$
$(a_{22})_n$	$Y^2 \left( \frac{1}{M^2} - \frac{m^2}{M^4} \right)$
$(a_{23})_n = (a_{32})_n$	$Y \sqrt{\frac{m^2}{M^4} - \frac{m^4}{M^6}}$
$(a_{33})_n$	$\frac{m^2}{M^2}$

#### 4.5 Comparing Experimental and Simulation Results

While the fiber orientation for the experimental sample is useful by itself, for the purpose of this study it is most valuable and informative when compared to predicted values in order to

refine the prediction methodology to more accurately represent actual behavior. There are four primary aspects that were considered when developing the comparison approach: quantitative and qualitative comparison and local and global understanding. The varying tensor calculation region, discussed previously in Section 4.2, provides the foundation for determining the overall local or global representation of the results but the quantitative versus qualitative understanding is more dependent on how the results are presented.

**Quantitative and Qualitative Comparison.** By measuring fiber orientation information for both experimental and predicted samples, a wide variety of both quantitative and qualitative comparisons can be made. Examples of qualitative comparisons include determining geometry changes that lead to divergence between predicted and actual fiber orientation, understanding how long after geometry changes it takes fibers to reach reasonable alignment, discovering limits for processing conditions at which prediction performance diminishes. When fiber orientation tensor values are known, quantitative values can be determined or assigned for each of these qualitative comparisons and have potential uses such as calculating the ratio between the change in angle for a geometry and the rate of prediction divergence, measuring the distance to reasonable alignment from a point of interest, or determining bias values based on processing conditions. Therefore, having measured fiber orientation values across a large sample region allows for powerful quantitative and qualitative comparisons that can be useful for designers and in the development of tools to integrate experimental studies with simulations for more accurate and useful predictions.

**Local and Global Understanding.** By designing the image processing framework to locate fibers even at low magnification, much larger sample cross-sections can be used to form a much more global representation of fiber orientation over complicated geometries. Recent work with fiber orientation has trended towards much more precise understanding of fiber orientation using very high magnification sources such as SEM. While this is very useful for understanding how to improve fiber orientation prediction and are invaluable to improving simulation predictions, this has a very limited understanding of the overall fiber orientation behavior in sample geometries. This study makes use of relatively low-magnification imaging and widely-used image processing software to create a more global perspective of the fiber orientation in sample geometries. While these techniques do not necessarily have the same accuracy as high-magnification methods, the loss in accuracy is made up for by having a much more complete understanding of the overall fiber orientation behavior and how it potentially affects simulation predictions, processing decisions, and design choices.

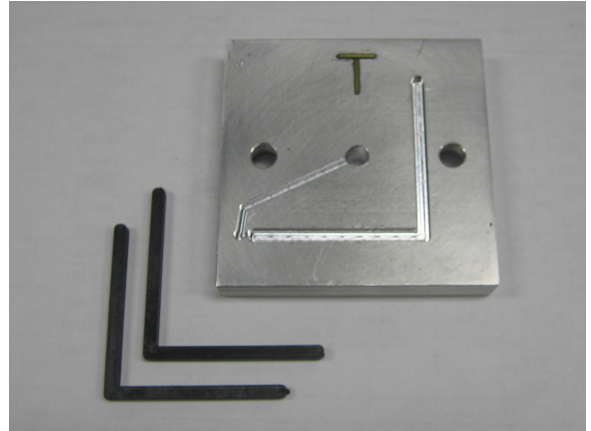


FIGURE 8: L-Channel mold with parts.

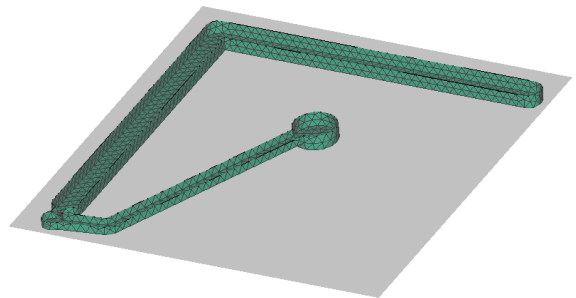


FIGURE 9: Sectioning plane for test geometry.

#### 4.6 Experiment Details

**Test Geometry.** An L-channel shape was chosen due to the highly uncertain behavior that occurs in the corner region and its prevalence in component design and specifically heat exchanger design. This geometry is useful for understanding how processing conditions and geometric properties can affect fiber orientation behavior in a drastic flow change and determining more complex phenomena such as how far from the corner it takes for the fiber orientation behavior to settle to a more consistent and well-aligned situation. This test geometry along with part of the injection mold used to create it are shown in Figure 8.

**Test Material.** In order to most accurately reflect the behavior of the proposed heat exchanger design, the material selected for the proposed design was used for this test geometry. This material is a commercially-available carbon-fiber filled Nylon 12, PolyOne NJ-6000 TC Black. The manufacturer-recommended injection molding processing conditions along with the injection molding machine specifications were used to determine the processing conditions for manufacturing the test samples, detailed in Table 2.

**Experimental Procedure Details.** The cross-section at the midplane of the longest direction, demonstrated in Figure 9, was

**TABLE 2:** Processing conditions for test sample.

Processing Condition	Value	Units
Injection Pressure	164	MPa
Injection Flow Rate	12	cm <sup>3</sup> /s
Melt Temperature	285	°C
Mold Temperature	30	°C

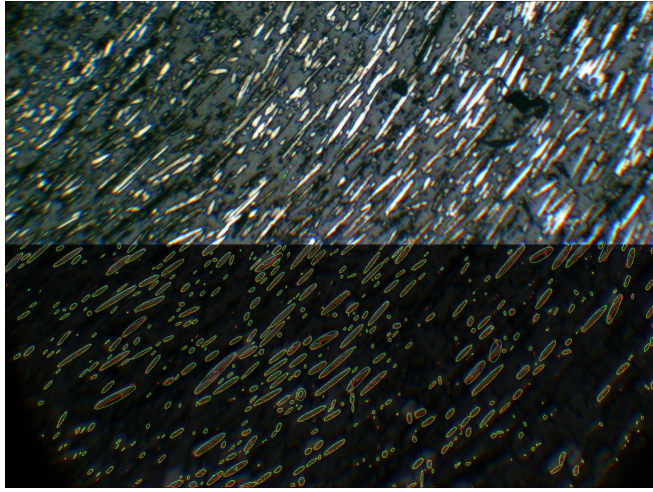


**FIGURE 10:** Example of collected microscope image with image processing results overlaid on lower half.

chosen because it provided the most information on the overall fiber orientation of the geometry in a single cross-section, a goal of the developed approach. A polishing apparatus was constructed to provide a precise polishing base and improve surface uniformity and quality and the polishing routine described in Section 4.1 was utilized to polish the experimental samples. With the sample sectioned and polished, it was microscope imaged to collect raw fiber orientation information. Based on an exploratory analysis, a microscope setup was chosen that supplied the most contrast between the fibers and surrounding matrix, with the fibers reflecting the supplied light and appearing white in the collected images and the matrix absorbing the supplied light and appearing black. Based on this procedure, Figure 10 demonstrates a microscope image collected for the test section.

## 5 RESULTS AND DISCUSSION

**Simulation Framework.** Using the processing conditions outlined in Table 2, Moldflow<sup>®</sup>, the industry-standard injection

molding simulation tool, was used to predict fiber orientation in the sample L-channel geometry. The fiber orientation analysis component of Moldflow<sup>®</sup> presents the results as either the three principle tensor values or the six tensor components in the global coordinate frame. The principle tensor values are a representation of the fiber orientation tensor in a special coordinate system in which the shear tensor components ( $t_{xy}$ ,  $t_{xz}$ , and  $t_{yz}$ ) are zero and is useful for gaining an understanding of the magnitude of the primary tensor components with respect to the polymer flow. For this study, the calculated tensor components are determined with respect to the global coordinate frame and therefore the primary tensor values can not be used and rather the full tensor component representation must be used.

Figure 11 shows the tensor components in the corner region of the L-channel geometry in which the polymer flow experiences a significant velocity change, which is the condition under which a higher level of uncertainty is expected in the predicted fiber orientation values. Thus, it provides the best location to compare the predicted fiber orientation tensor values with the measured ones. To create a continuous representation of the tensor components at this location, multi-linear interpolation on the calculated tensor components at each node. This is useful for the comparison framework because the tensor values can be determined for any tensor region regardless of its size and position.

**Comparison Results.** The L-channel was sampled at 5x magnification and analyzed across the shown region. A sample image with the processed results is shown below. The image processing framework was effective in identifying most of the fibers in the sample images and was used to successfully develop tensor plots for comparison to Moldflow<sup>®</sup> results.

First, a more global understanding of the fiber orientation behavior in the corner region of the L-channel was investigated. Figure 12 shows the experimental measurements with a relatively coarse tensor region size substituted for overlayed the Moldflow<sup>®</sup> predictions in Figure 11, where the Moldflow<sup>®</sup> predictions are retained where the flow enters from the top of the corner and exits to the left. Only the primary tensor components,  $t_{xx}$ ,  $t_{yy}$ ,  $t_{zz}$ , and  $t_{xy}$ , are shown since they are most representative of the fiber orientation in this region and it is not possible to resolve the signs for the remaining out-of-plane components. In the color scale, blue represents a component value of 0 (no alignment) and red represents 1 (full alignment).

It is shown that throughout the sample, the level of correlation varies greatly. There are regions which the predicted and experimental values match closely and others which the values diverge greatly. Although this result is significant, it should not be assumed that either the Moldflow<sup>®</sup> prediction is incorrect or the measurement is invalid. The L-channel geometry was chosen specifically due to the very high uncertainty that occurs in the sharp velocity change and the difficulty that arises in simulating this behavior. Therefore, these findings do not suggest that there are underlying flaws in the employed Moldflow<sup>®</sup> fiber orienta-

tion models, just limitations in highly uncertain flow situations for which predictions may be insufficient and measured values should be used instead.

The primary out-of-plane fiber orientation tensor component,  $t_{zz}$ , is negligible in the Moldflow® predictions but not in the experimental findings. This signifies an important design improvement in the out-of-plane thermal performance and could lead to improved application results compared to the simulation predictions. The conservative fiber orientation models did not predict out-of-plane orientation for the in-plane velocity change and therefore design changes that could have been introduced to improve out-of-plane alignment would not have registered in simulation predictions. This represents the importance of incorporating experimental fiber orientation measurements during the design phase to ensure the heat exchanger that best utilizes fiber orientation can be created.

Next, the exit region of the test sample was investigated using a high-resolution tensor region, shown in Figure 13. This investigation allows for a more detailed comparison of the Moldflow® predictions and experimental values both for the exit orientation and the transition within the corner region. Again, differences between predicted and measured values should not be used to disregard either value. Instead, experimental findings can be used to bias or refine predictions in certain geometries and other instances in which it is found that they diverge.

Based on the findings shown in Figure 13, the following general conclusions can be drawn for this example. Insufficient fiber information was collected along the left edge of the region to accurately determine tensor components for the left-most tensor regions. The primary out-of-plane tensor component,  $t_{zz}$ , shows little variation across the section but the simulation predictions are too conservative in assuming no out-of-plane alignment and there is poor agreement with the measured values.  $t_{xx}$  and  $t_{yy}$  correspond most directly with the direction of flow for the polymer and show relatively poor agreement in the central region at the exit of the corner while the surface areas at the inside and outside of the corner have strong agreement between predicted and measured values. This indicates a high level of uncertainty at locations away from the mold walls and generally increasing uncertainty with increasing radius from the interior of the corner. For this example, it would be valuable to use experimentally measured values for centrally located regions in geometries with rapid velocity changes while predicted values should be sufficient for the remainder of the test region. Qualitatively though, all of the experimental components appear to show variations within this region that are similar to the predictions, which indicates that it is possible to utilize the Moldflow® simulations to understand the effects of molding features on relative changes in fiber orientation. However, more accurate absolute quantification using the simulations does not appear to be feasible.

## 6 CONCLUSIONS

Thermally-enhanced and other fiber-filled composites that have been introduced into the polymer marketplace can lead to dramatic improvements in material properties, including thermal conductivity and structural factors, but these properties are affected by the fiber orientation within the component. This study presents an approach to experimentally measure and calculate the fiber orientation information for sample parts and demonstrates a comparison framework for comparing measured values to fiber orientation values predicted by the industry-standard injection molding simulation tool Moldflow®.

Previous work in experimentally determining fiber orientation was found to have three primary focuses when developing experimental methodologies: sectioning techniques, imaging methods, and image processing algorithms. The developed method successfully measured fibers in a simple section using traditional light microscopy and relatively low magnification and calculated fiber orientation tensor values at both high and low resolution for both a global and local understanding of fiber orientation. This allows the method to be applied to a range of fiber orientation measurement applications and reduces many barriers to implementation in many environments.

This study successfully developed a fiber orientation measurement framework for comparing experimental results to simulation predictions for injection molded thermally-enhanced polymers. This is useful for studying advanced materials for which the applicability of more traditional prediction tools is unknown. Additionally, the flexibility of the developed method allowed large sections to be studied while determining fiber orientation at granular levels to develop both a global and local understanding of fiber orientation in the test sample. The tool uses traditional tools and open source methods to maintain availability for broad audiences. The developed method is useful for overall testing, such as manufacturing verification of expected overall fiber orientation in sample parts and is useful for determining a qualitative understanding of the fiber orientation behavior as well as generating qualitative results for direct comparison to simulation results.

## ACKNOWLEDGMENTS

This research was performed as part of the Energy Education and Research Collaboration (EERC) between the University of Maryland and The Petroleum Institute. The authors would like to thank the Abu Dhabi National Oil Company (ADNOC) and its international partners for their generous financial support.

## REFERENCES

- [1] Luckow, P., Bar-Cohen, A., Rodgers, P., and Cevallos, J., 2010. "Energy efficient polymers for gas-liquid heat ex-

- changers". *J. of Energy Resources Technology*, **132**(2). DOI: 10.1115/1.4001568.
- [2] T'Joen, C., Park, Y., Wang, Q., Sommers, A., Han, X., and Jacobi, A., 2009. "A review on polymer heat exchangers for HVAC&R applications". *International J. of Refrigeration*, **32**(5), pp. 763–779. DOI: 10.1016/j.ijrefrig.2008.11.008.
- [3] Bar-Cohen, A., Rodgers, P., and Cevallos, J., 2008. "Application of thermally enhanced thermoplastics to seawater-cooled liquid-liquid heat exchangers". In Proceedings 5th European Thermal-Sciences Conference.
- [4] Folgar, F., and III, C. L. T., 1984. "Orientation behavior of fibers in concentrated suspensions". *J. of Reinforced Plastics and Composites*, **3**.
- [5] Advani, S. G., and III, C. L. T., 1987. "The use of tensors to describe and predict fiber orientation in short fiber composites". *J. of Rheology*, **31**, pp. 751–784.
- [6] Robb, K., Wirjadi, O., and Schladitz, K., 2007. "Fiber orientation estimation from 3D image data: Practical algorithms, visualization, and interpretation". In Seventh International Conference on Hybrid Intelligent Systems. DOI: 10.1109/HIS.2007.26.
- [7] Clarke, A. R., Archenhold, G., and Davidson, N. C., 1995. "A novel technique for determining the 3D spatial distribution of glass fibres in polymer composites". *Composites Science and Technology*, **55**, pp. 75–91.
- [8] Fischer, G., and Eyerer, P., 1988. "Measuring spatial orientation of short fibre reinforced thermoplastics by image analysis". *Polymer Composites*, **9**, pp. 297–304.
- [9] Hine, P. J., Duckett, R. A., Davidson, N., and Clarke, A. R., 1993. "Modelling of the elastic properties of fibre reinforced composites. I: Orientation measurement". *Composites Science and Technology*, **47**.
- [10] Davidson, N. C., Clarke, A. R., and Archenhold, G., 1997. "Large-area, high-resolution image analysis of composite materials". *J. of Microscopy*, **185**, pp. 233–242.
- [11] Lee, Y. H., Lee, S. W., Youn, J. R., Chung, K., and Kang, T. J., 2002. "Characterization of fiber orientation in short fiber reinforced composites with an image processing technique". *Materials Research Innovations*, **6**, pp. 65–72. DOI: 10.1007/x10019-002-0180-8.
- [12] Zak, G., Park, C. B., and Benhabib, B., 2001. "Estimation of three-dimensional fibre-orientation distribution in short-fibre composites by a two-section method". *J. of Composite Materials*, **35**, pp. 316–339. DOI: 10.1177/002199801772662190.
- [13] Bay, R. S., and III, C. L. T., 1992. "Stereological measurement and error estimates for three-dimensional fiber orientation". *Polymer Engineering and Science*, **32**.
- [14] Kim, E. G., Park, J. K., and Jo, S. H., 2001. "A study of fiber orientation during the injection molding of fiber-reinforced polymeric composites (comparison between image processing results and numerical simulation)". *J. of Material Processing Technology*, **111**, pp. 225–232.
- [15] Akay, M., and Barkley, D., 1991. "Fibre orientation and mechanical behavior in reinforced thermoplastic injection mouldings". *J. of Materials Science*, **26**, pp. 2731–2742.
- [16] Régnier, G., Dray, D., Jourdain, E., Roux, S. L., and Schmidt, F. M., 2008. "A simplified method to determine the 3D orientation of an injection molded fiber-filled polymer". *Polymer Engineering and Science*. DOI: 10.1002/pen.21161.
- [17] Eberhardt, C., and Clarke, A., 2001. "Fibre-orientation measurements in short-glass-fibre composites, Part I: Automated, high-angular-resolution measurement by confocal microscopy". *Composites Science and Technology*, **61**, pp. 1389–1400.
- [18] Hemsley, D. A., ed., 1989. *Applied Polymer Light Microscopy*. Elsevier Applied Science, London.
- [19] Sawyer, L. C., and Grubb, D. T., 1996. *Polymer Microscopy*. Chapman & Hall, London.

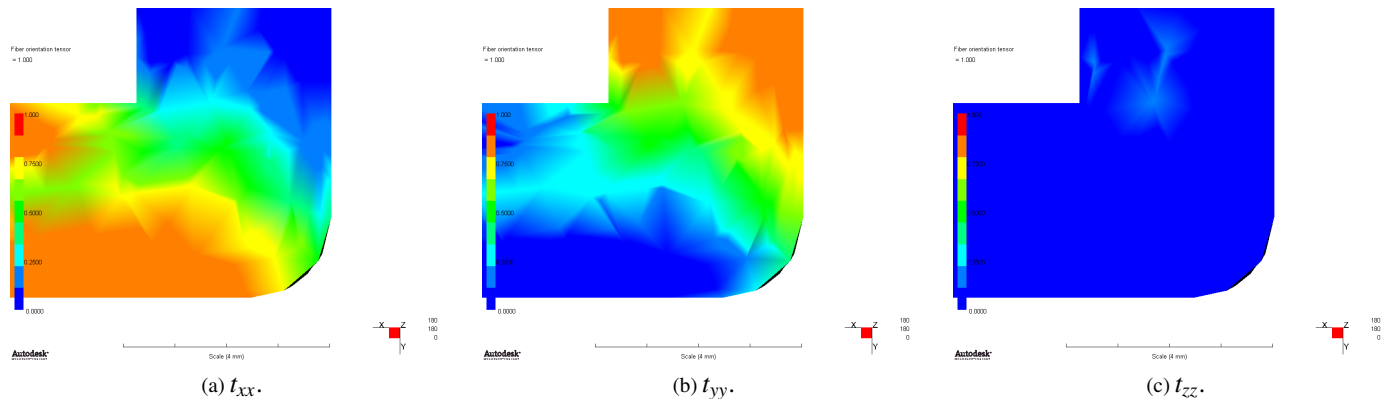


**FIGURE 11:** Moldflow® tensor component results.

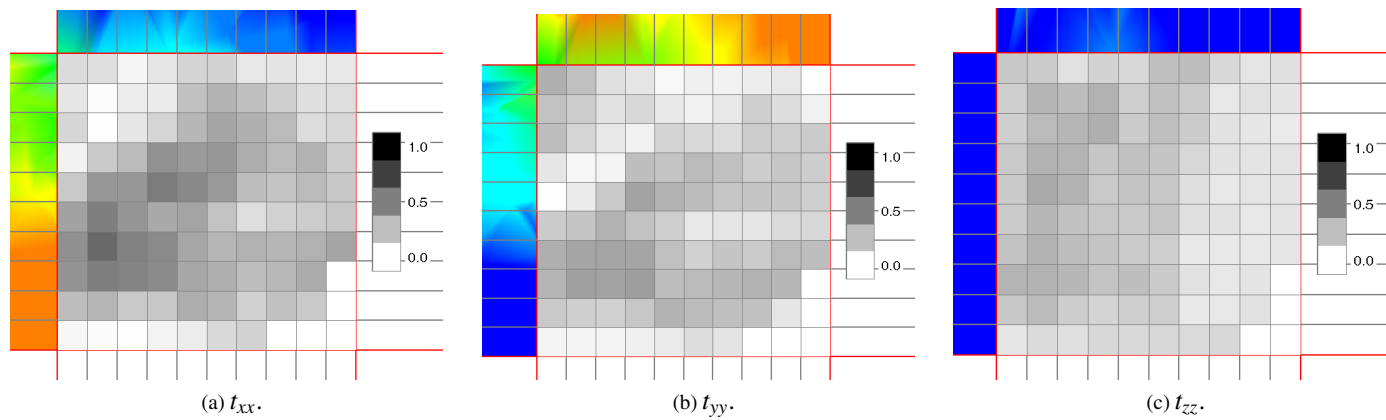


**FIGURE 12:** Tensor results.

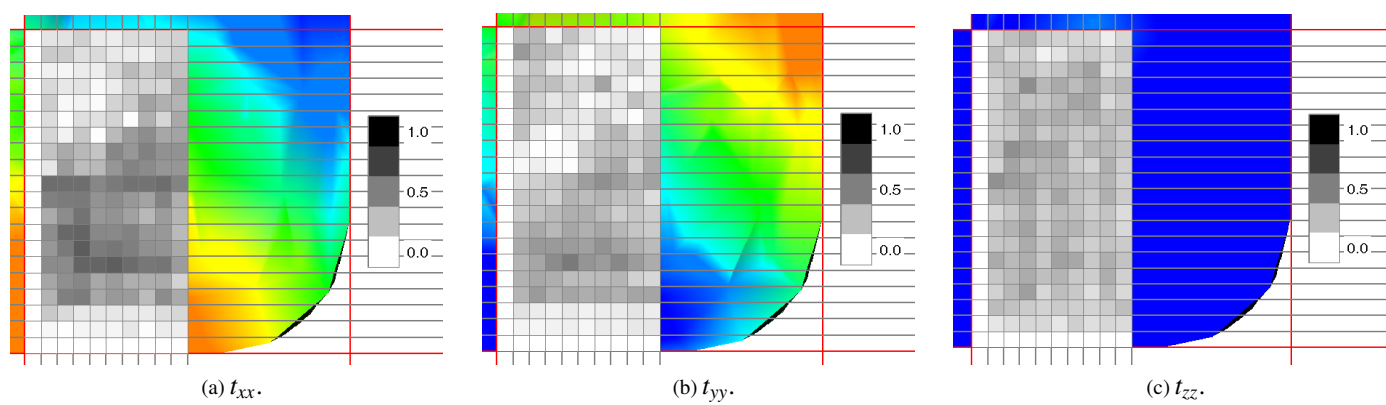


**FIGURE 13:** Detailed tensor results.